STATISTICAL ESTIMATES OF ROCK-FREE LUNAR REGOLITH THICKNESS FROM DIVINER. J. Venkatraman[1] and D. A. Paige[1], [1]Department of Earth, Planetary and Space Sciences, UCLA, LA, CA 90095 (jaahnavee96@ucla.edu).

Introduction: With virtually no atmosphere, the moon preserves evidence on its surface that has implications for remote sensing studies [1], subsurface volatile research [2], and landing site determination [3]. In the past, the thickness of the lunar surface regolith has been approximated using seismic data [1], radar data [4], and crater size frequency distribution statistics [5] to be on the order of tens of meters. Here we estimate rock-free regolith thickness statistically using the LRO Diviner Lunar Radiometer [6] rock abundance estimates from cold spot craters.

Surface temperatures from derived Diviner thermal measurements allow us to map rock abundance (areal fraction of boulders, meter-sized and larger, present in a Diviner pixel) [7] on the lunar surface. We expect that larger craters will excavate deeper into the lunar surface, and we can measure lunar regolith thickness as the smallest depth at which these craters hit consolidated rock detectable by Diviner. Since rock abundance signatures have been shown to fade over time [8], we focus on fresh craters which are well constrained by cold spots on the lunar surface [9, 10].

Methods: We use the cold spot dataset from [10], covering equatorward of ± 50 degrees latitude, with over 2200 cold spot craters, ranging from 43 m to 2.3 km in diameter. We identify the center of each cold spot crater in both LROC (Lunar Reconnaissance Orbiter Camera) images [12] and Diviner 128 ppd global rock abundance maps [7, 11]. Using our own code, we calculate the values of maximum and mean rock abundance for each crater's interior and surrounding ejecta within three radii from the center of that crater as shown in Figure 1. We then normalize rock abundance (NRA) calculated as maximum minus mean rock abundance to account for the right-skew of crater ejecta rock abundance distributions [8].

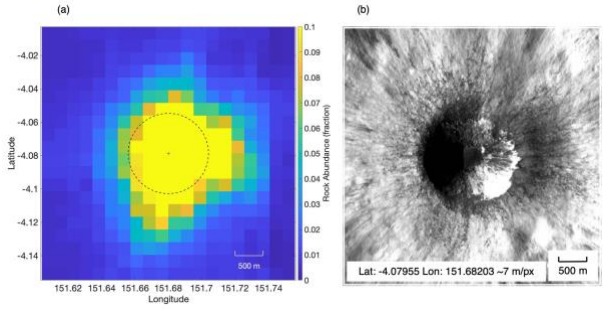

Figure 1: (a) Example cold spot crater on the Diviner rock abundance maps where each pixel corresponds to a different value of rock abundance. The black dashed line represents the rim of the crater centered at '+'. The plot extends out to three radii from the center of this crater. (b) LROC image of the same crater three radii out from the center.

Excavation Depth Calculations: There are numerous processes that tend to affect the depth of a crater, including ejection and displacement of crater material, and formation of a transient crater. Below a diameter of approximately 130 m, the d/D (apparent depth/apparent diameter) ratio gradually decreases further due to gravity dominated slumping and collapse of smaller, weaker crater walls [13]. Therefore, what we are truly interested in is depth of excavation (d_e) as opposed to apparent depth of the crater. Melosh [14] indicates that depth of excavation of simple craters with an apparent diameter (D) < 15 km is 10% of the diameter of the transient crater (D_t), which is 84% of the apparent diameter of the crater.

$$d_e \approx 0.1\, D_t \quad (1)$$
$$D_t = 0.84\, D \quad (2)$$
$$d_e \approx (0.84)(0.1)\, D = 0.084\, D \quad (3)$$

Using Melosh's estimates, we get a depth of excavation equal to 8.4% of the apparent diameter of a small, simple crater.

Results: Our approach for identifying rocky craters requires choosing a 'rockiness' decision threshold, below which craters are considered not rocky and above which they are considered rocky. A threshold of 0.3 % NRA is selected, and the probability that a given crater has an NRA value greater than 0.3 % is defined as the rockiness fraction.

In Figure 2, we plot the rockiness fraction against crater diameter and excavation depth. The rockiness fractions for both the mare and highlands roughly follow Gaussian CDFs, the fits to which have means of 150 and 220 m respectively. If half the craters in a particular diameter bin are rocky (rockiness fraction = 0.5), we consider this to be an indication of rock excavation detectable by Diviner. The results show that 50 % of craters are rocky at a diameter of 150 m in the mare, and 220 m in the highlands. In accordance with Melosh [14], these correspond to excavation depths of 12.6 and 18.5 m respectively. Lunar mare craters seem, on average, to become rocky at far shallower depths than those on the highlands.

The difference in standard deviations between the mare and highlands regions (Figure 2) is also of particular significance. The highlands distribution fit

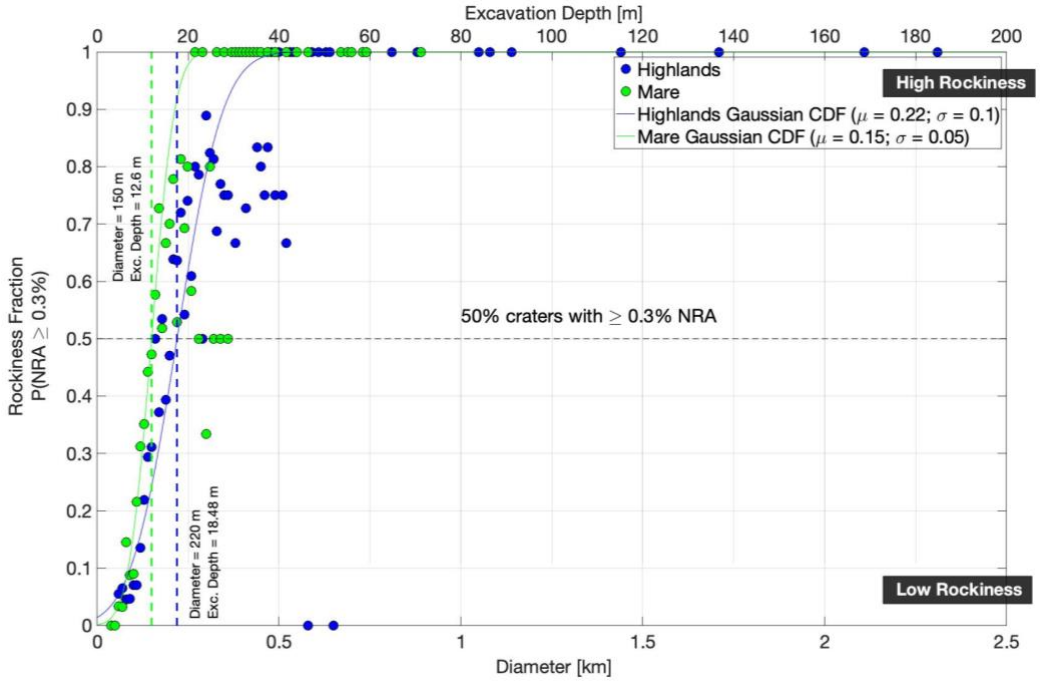

Figure 2: Rockiness fraction by crater diameter (bin width 0.01 km) and excavation depth for the lunar mare and highlands. The y-axis ranges from 0 = 'Low Rockiness', to 1 = 'High Rockiness'. Each green and blue marker represents P(NRA ≥ 0.3 %) for each diameter bin in the mare and highlands respectively. The green and blue solid curves are theoretical Gaussian CDFs for those regions. The black dashed line is the point at which 50 % or more of the craters in a given bin have an NRA ≥ 0.3 % (rockiness fraction = 0.5).

has a standard deviation 50 m greater than that of the mare. We see this represented visually in the greater spread of the highlands rockiness fractions across crater diameter and excavation depth as compared to the mare.

Discussion: Our excavation depth results give us unique values for both the mare and the highlands regions, however interpreting these results in terms of a single regolith thickness can be problematic. Firstly, regolith thickness estimates are not only varied across techniques, but also spatially within smaller regions on the lunar surface. Secondly, we must rely on existing excavation depth models [14]. Sharpton [15] has suggested a new model based on higher resolution LROC images showing crater deformation that suggest a depth of excavation less than or equal to 3 % of the diameter of the transient crater.

$$d_e \leq 0.03\ D_t \quad (4)$$

$$\Rightarrow d_e \approx (0.84)(0.03)\ D = 0.025\ D \quad (5)$$

Using Sharpton's results would give a depth of excavation of 2.52 % of the apparent diameter of a small, simple crater. Melosh's model [14] three times those of Sharpton's [15]. However, both models give us estimates that are within the range of other previous estimates [1, 4, 5].

References: [1] F. Hörz et al. (1991). *Lunar Sourcebook, 340,* 61-111. [2] L. Rubanenko et al. (2019). *Nature Geoscience, 12(8),* 597–3756. [3] G. J. Taylor (1985). [4] Y. G. Shkuratov and N. V. Bondarenko (2001). *Icarus, 149(2),* 329-338. [5] B. B. Wilcox et al. (2005). *Meteoritics & Planetary Science, 40(5),* 695-710. [6] D. A. Paige et al. (2010). *Space Science Reviews, 150,* 125-160. [7] J. L. Bandfield et al. (2011). *JGR, 116.* [8] R. R. Ghent et al. (2014). *Geology, 42(12),* 1059-1062. [9] J. L. Bandfield et al. (2014). *Icarus, 231,* 221-231. [10] J. P Williams et al. (2018). *JGR, 123(9),* 2380-2392. [11] J. P. Williams et al. (2017). *Icarus, 283.* [12] M. S. Robinson et al. (2010). *Space Science Reviews, 150,* 81-124. [13] J. D. Stopar et al. (2017). *Icarus, 298,* 34-48. [14] H. J. Melosh (1989). *Planetary Surface Processes*. [15] V. L. Sharpton (2014). *JGR, 119(1),* 154-168. [16] J. Venkataraman and D. A. Paige (2021). *Mendeley.*

Acknowledgments: The NRA data used in this study is publicly available on Mendeley [16]. Other derived data products used are available via the Geosciences node of PDS (https://pds-geosciences.wustl.edu/missions/lro/diviner.htm) and the LROC data node (http://lroc.sese.asu.edu/).